Available online at www.sciencedirect.com

ScienceDirect

Procedia Engineering 99 (2015) 368 – 376

Procedia Engineering

www.elsevier.com/locate/procedia

"APISAT2014", 2014 Asia-Pacific International Symposium on Aerospace Technology, APISAT2014

The Numerical Simulation of Civil Transportation High-lift Configuration

Hao Xuan*, Su Cheng, Hu Ning, Zhang weimin

China Academy of Aerospace Aerodynamics, 17 Yungang West Road, Beijing, 100074, P. R. China

Abstract

The complex multiform flow phenomenon including boundary layer transition, lamination separation, turbulence attach line and re-lamination, boundary shock interaction and so on will appear when the air flow over the high lift configuration, which makes it very difficult to predict by numerical simulation. In order to validate the CFD code prediction capability of high lift configuration of swept wing with high aspect ratio, AIAA held two workshops of CFD high lift prediction in 2010 and 2012. The NASA Trap wing model and DLR-F11 model were chosen to research the mesh resolution, turbulence model, transition prediction and Reynolds effect by numerical simulation. Based on the published work of the1st and 2nd high lift prediction workshop, some numerical simulation research to validate the rationality of mesh generation are done in this paper. The two configurations of NASA Trap wing and DLR F-11 are simulated by solving the Reynolds-averaged Navior-Stokes equations with the S-A turbulence model. The numerical data in linear region agree very well with the experiments but the discrepancy between numerical data and experiment data near the stall region is perceptible. It can be conclude generally from the numerical results of two configurations that in the engineer design phase the Reynolds-averaged Navior-Stokes equations can give correct results of the aerodynamic characteristic with carefully generated mesh and appropriate turbulence model.

Peer-review under responsibility of Chinese Society of Aeronautics and Astronautics (CSAA)

Keywords: High lift Device; Numerical Simulation; Trapwing; DLR F-11

* Corresponding author. Tel.: +86-13810025289
E-mail address: haoxuan0722@sohu.com

Peer-review under responsibility of Chinese Society of Aeronautics and Astronautics (CSAA)
doi:10.1016/j.proeng.2014.12.549

1. Introduction

The high lift device is one of the most important parts during the civil transportation taking off and landing and has a direct relationship to the reliability, economy and environment protecting of the aircraft. The configuration and flow field of the high lift device is very complicated with the flow phenomenon including boundary layer transition, lamination separation, turbulence attach line and re-lamination, boundary shock interaction and so on when the air flow over the high lift configuration, which makes it very difficult to predict by numerical simulation. The maximum lift coefficient and stall angle of the transportation aircraft during the civil transportation taking off and landing are the two key parameters of high lift device design. Limited by the turbulence model, simulation method and so on, it is difficult to get these parameters accurately by CFD (Computational Fluid Dynamics) simulation. Although as the rapid development of computer, the application of CFD during the aircraft aerodynamic design are more and more popular, the computation of high lift flow is still a big challenge.

In order to develop the proper numerical method, turbulence model and mesh generation standard of high lift configuration of swept wing with high aspect ratio and comprehend the physics of high lift flow expressly, AIAA held two workshops of CFD high lift prediction in 2010 and 2012. The NASA Trap wing model and DLR-F11 model were chosen to research the mesh resolution, turbulence model, Reynolds effect, transition prediction and geometry details by numerical simulation. Based on the published work of the1st and 2nd high lift prediction workshop[1]-[5], some numerical simulation research of Trapwing and DLR-F11 model are done in this paper, with the emphases to validate the rationality of mesh generation.

2. Numerical Methods

The steady Reynolds averaged Navior-Stokes equation is chosen in this paper to solve the high lift flow field full turbulently with SA turbulence model. In inertial Cartesian coordinates, the integration form of the steady N-S equation can be written as:

$$\frac{\partial}{\partial t}\iiint_{\Omega}\overline{Q}d\Omega+\iint_{S}\left(\overline{G}-\overline{Q}\vec{q}_{b}\right)\cdot d\vec{S}=\frac{1}{\mathrm{Re}}\iint_{S}\overline{F}^{V}\cdot d\vec{S} \tag{1}$$

$$\overline{Q}=\begin{bmatrix}\rho\\ \rho u\\ \rho v\\ \rho w\\ \rho e_{t}\end{bmatrix},\quad \overline{G}=\begin{bmatrix}\rho u & \rho v & \rho w\\ \rho u^{2}+p & \rho vu & \rho wu\\ \rho uv & \rho v^{2}+p & \rho wv\\ \rho uw & \rho vw & \rho w^{2}+p\\ \rho uh_{t} & \rho vh_{t} & \rho wh_{t}\end{bmatrix},\quad \overline{F}^{V}=\begin{bmatrix}0 & 0 & 0\\ \tau_{xx} & \tau_{yx} & \tau_{zx}\\ \tau_{xy} & \tau_{yy} & \tau_{zy}\\ \tau_{xz} & \tau_{yz} & \tau_{zz}\\ \varphi_{x} & \varphi_{y} & \varphi_{z}\end{bmatrix}, \tag{2}$$

The $\overline{G}$, $\overline{\mathrm{F}}^{\mathrm{V}}$ is convention term and dispersion term separately, where Ω is the control volume. S is the control surface, and $d\vec{S}$ is the out normal surface vector of the S.

3. Numerical Results and Analysis

3.1. NASA Trapwing model

3.1.1Model

The Trapwing model in the wind tunnel is showed in Fig. 1. The config1 in test cases with full spanwise flap deployed at 25 degree and slat deployed at 30 degree is simulated. The main geometry parameters are listed in Tab. 1.

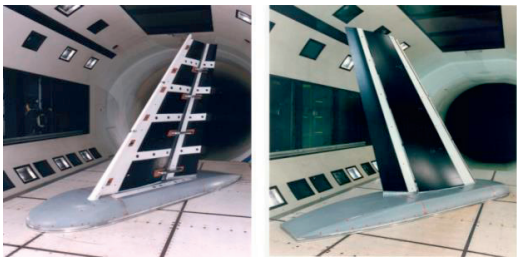

Fig. 1 NASA Trapwing model

Tab. 1 Trapwing geometry parameter

half span	85.05 inch
wing reference area	22.03 feet^2
reference chord	39.6 inch
aspect ratio	4.56
taper ratio	0.4
1/4 chord sweep	30 egree

3.1.2.Mesh Generation

(a) Structured Mesh

The structured mesh is generated by ICEM. The initial spacing normal to the viscous wall of the O grid is 3×10^{-6} meter with the value of y^+ 0.7, and the growth rate in the viscous layer is 1.18. The number of O grid points normal to the wall is 33 and the total number of the grid is about 30 million. Fig. 2 is the structured mesh distribution of Trapwing model.

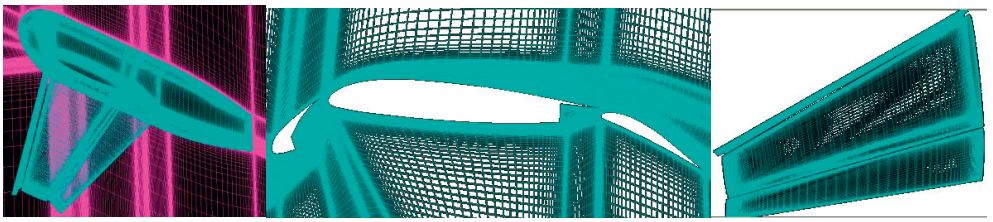

Fig. 2 The structure mesh distribution of Trapwing model

(b) Unstructured Mesh

The unstructured mesh is generated by ICEM. The prism mesh is generated around the viscous wall to catch the flow details in the boundary layer with the initial spacing 3×10^{-6} meter. The growth rate of the prism mesh is 1.18 with the number of the prism grid points normal to the wall 30 and height 0.00254 meter. The total number of the mesh is 49.4 million. Fig. 3 is the unstructured mesh distribution of Trap wing model.

Fig. 3 The unstructured mesh distribution of Trapwing model

3.1.3.Numerical Results and Analysis

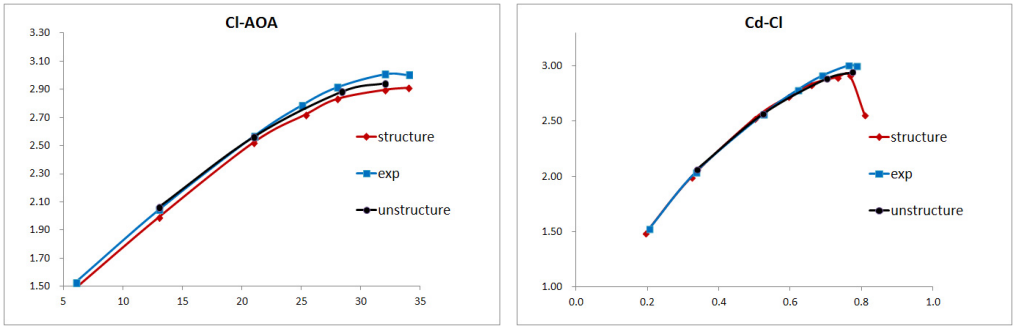

Fig. 4 Lift and drag curves of Trapwing model

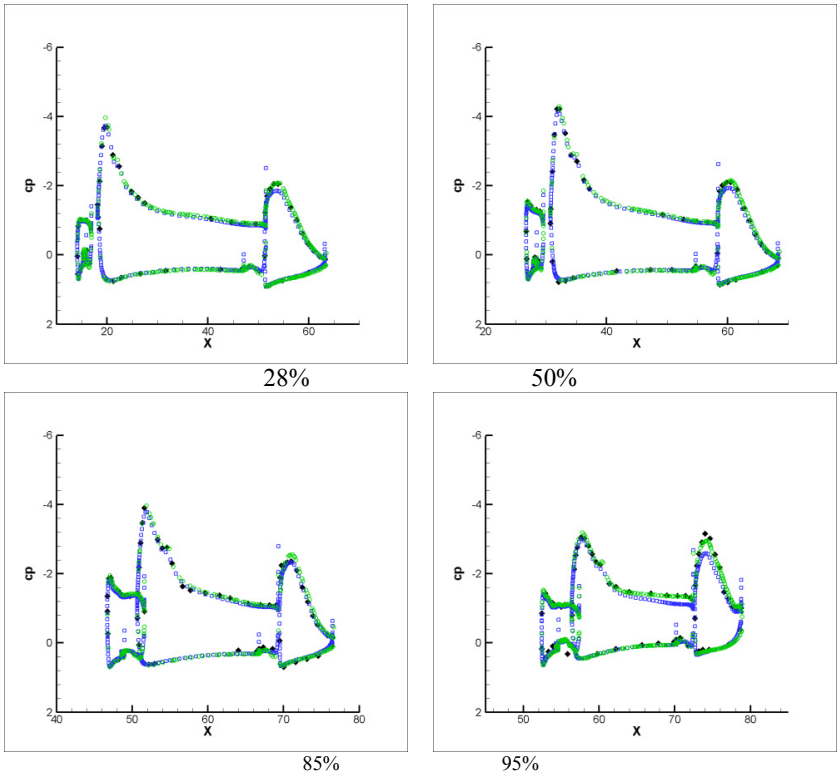

AOA=13

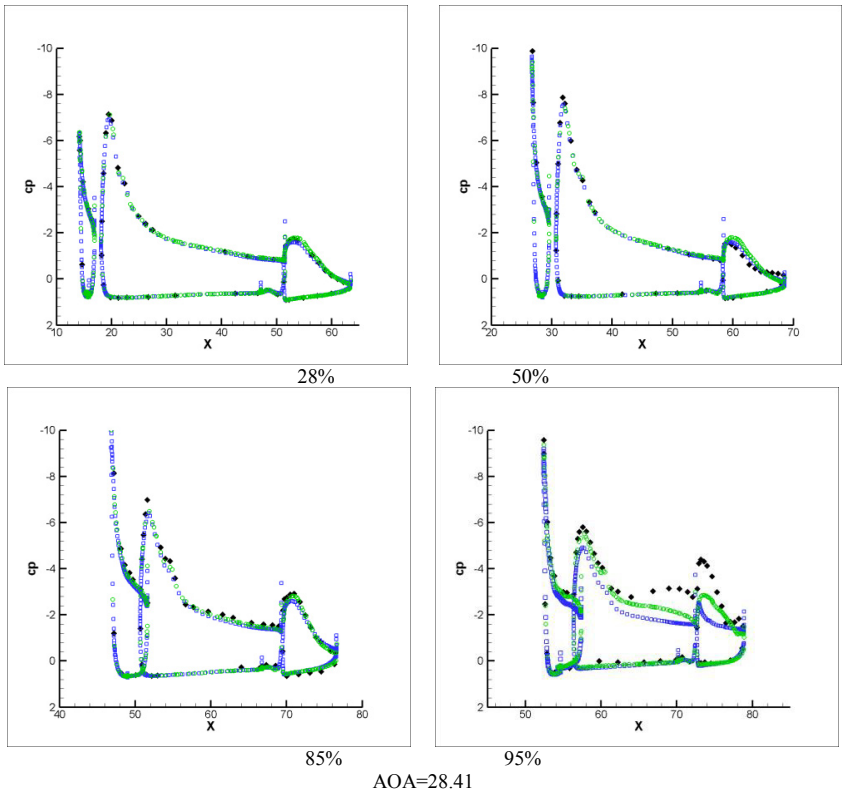

AOA=28.41

（black diamond: experiment; blue square: structured grid; green circle: unstructured grid）

Fig. 5 Surface pressure coefficient of Trapwing model

The structured and unstructured meshes are uses to simulate the flow field separately with the S-A turbulent model. The Mach number is 0.2 and the corresponding Reynolds number is 4.3×10^6. Fig. 4 shows lift and drag coefficients comparison between the simulation of structured grid, unstructured grid and experiments. It can be seen from the lift curve that the numerical result agrees well with the experiment results in the linear region but some discrepancy can be found distinctly in the non-linear region, which can also be seen from the polar curve. The discrepancy between numerical results and experiment results is mainly caused by the insufficiency of turbulent model to simulate the stall and the full turbulent simulation without considering the transition influence [1]. （black diamond: experiment; blue square: structured grid; green circle: unstructured grid）

Fig. 5 gives the surface pressure coefficient alone the span wise at the angle of attack13 degree and 28.41degree. It can be seen that both at the mid angle of attack in the linear region and large angle of attack in the non-linear region, the surface pressure coefficients of structured grid and unstructured grid agree well with the experiment from the root to the span wise of 80%. But there is a discrepancy between the numerical result and experiment result at the tip of the wing, which becomes more and more obvious as the angle of attack increase. At the angle of attack 13 degree, the discrepancy is mainly occurs at the trailing edge of the main wing and the leading edge of the flap, but at the angle of attack 28.41 degree the discrepancy extends to the trailing edge of slat, the full main wing and flap. As we know that the vortex at the wing tip will become stronger as the lift increase which leads to the increasing of the sensitivity of the flow field to mesh refinement. The accurate simulation of the flow field at wing tip requires a much fine mesh and a much applicable turbulent model.

3.2. DLR-F11 model

3.2.1 Model

Fig. 6 DLR-F11model

Fig. 6 shows the DLR-F11 model in the wind tunnel. A simple model is used in numerical simulation without considering slat track, flap track fairings and slat pressure tube bundles. Tab. 2 gives the geometry parameters of DLR-F11 model.

Tab. 2 DLR-F11 geometry parameters

half span	1.4m
wing reference area	$0.42m^2$
reference chord	0.347m
aspect ratio	9.35
taper ratio	0.3
1/4 chord sweep	30°
fuse length	3.077m
slat deployed angle	26.5°
flap deployed angle	32°

3.2.2 Mesh

(a) Structured Mesh

The structured mesh is generated by ICEM. The initial spacing normal to the viscous wall of the O grid is 10^{-6} meter with the value of y^+ 2. The number of O grid points normal to the wall is 33 with the growth rate in the viscous layer 1.25. The distribution of grid points around the slat, main and flap surface is 113×153、245×153、105×153 and the total number of the grid is about 30 million. Fig. 7 is the structured mesh distribution of DLR-F11 model.

(c) Unstructured Mesh

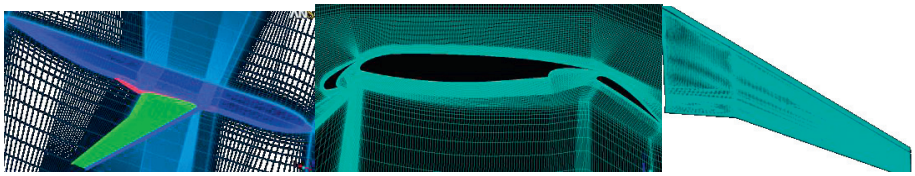

Fig. 7 The structure mesh distribution of DLR-F11 model

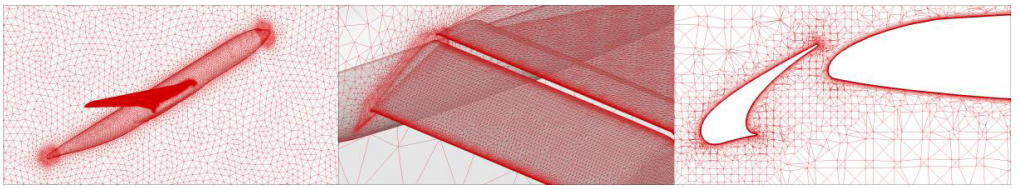

Fig. 8 The unstructured mesh distribution of DLR-F11model

The unstructured mesh is generated by ICEM. The prism mesh is generated around the viscous wall to catch the flow details in the boundary layer with the initial spacing 4-8×10^{-7} meter and the value of y^+ 0.7-1.2. The number of the prism grid points normal to the wall is 36 with growth rate of the prism mesh 1.2. The total number of the mesh is 31.7 million. Fig. 8 is the unstructured mesh distribution of Trap wing model.

3.2.3 Numerical Results and Analysis

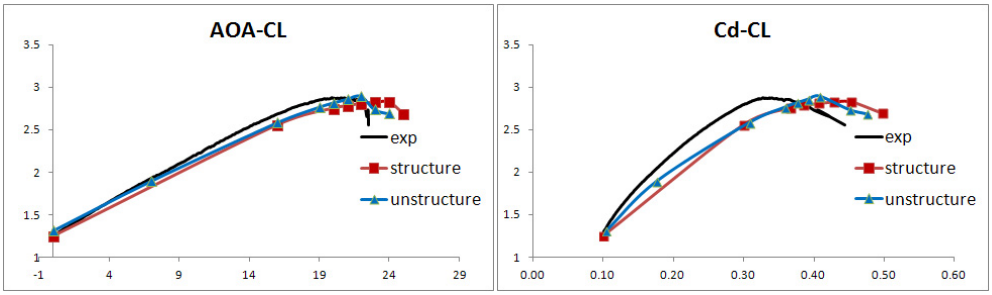

Fig. 9 Lift and drag curves of DLR-F11 model

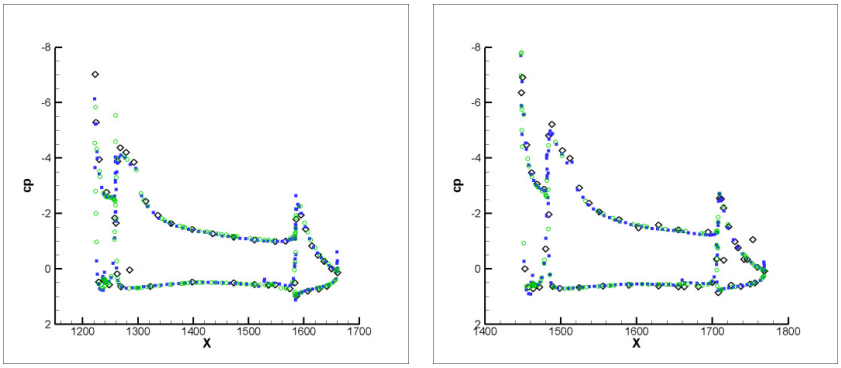

28.85% 54.3%

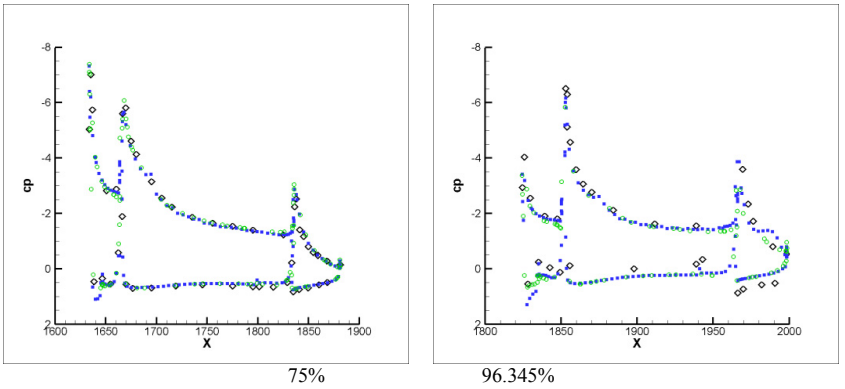

(a) AOA=16

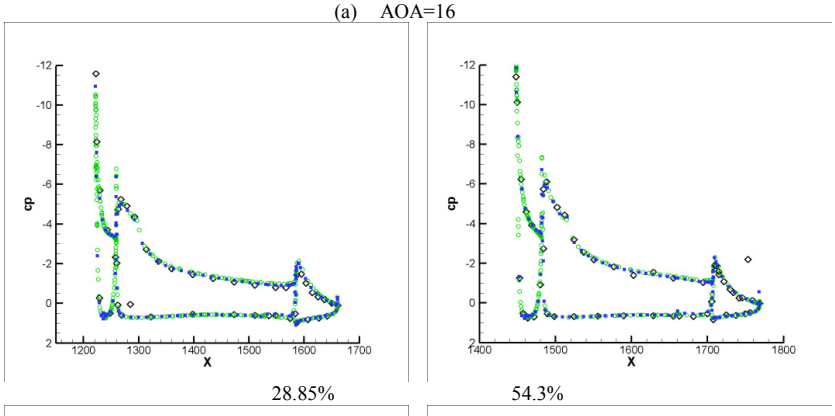

(b) AOA=21

(c) (black diamond: experiment; blue square: structured grid; green circle: unstructured grid)

Fig. 10 Surface pressure coefficient of DLR-F11model

The structured and unstructured meshes are uses to simulate the flow field separately with the S-A turbulent model. The Mach number is 0.175 and the corresponding Reynolds number is 15.1×10^6. Fig. 9 shows lift and drag coefficients comparisons between the simulation by structured grid, unstructured grid and experiments. It can be seen that there is a little different of the slope of lift coefficient curve between the numerical results and experiments results, which is likely to be caused by the discrepancy between the two model used in numerical simulation and experiments. The CFD results agree well with the experiment at low and middle angle of attack but in the non-linear region, the lift coefficient is small and the stall delays compared with the experiments. The maximum of lift coefficient of experiment is 2.873 with the stall angle 20 degree. The maximum of lift coefficient of numerical

simulation is 2.827 and 2.893 for structured grid and unstructured grid, and the stall angle is 24 and 22 degree, separately. The comparison of surface pressure coefficients at different span station at the angle of attack 16 degree and 21 degree between the numerical simulation of structured grid, unstructured grid and the experiment results are shown in (black diamond: experiment; blue square: structured grid; green circle: unstructured grid)

Fig. 10. It can be seen that the CFD results agree perfect with the experiment from the wing root to the outer part of the wing. At the wing tip, there is a distinct discrepancy of the surface pressure coefficient between the structure grid result and experiment, which is mainly caused by the not fine enough distribution of the mesh around the tip region. Based on the structure grid result, the unstructured grid is refined and a perfect result can be seen in the picture, which indicates the sensitivity of the flow field around wing tip to the mesh again.

4. Summary

In this paper, the aerodynamic characteristics of high lift models are researched by numerical simulation. The structured and unstructured grids are generated by ICEM. The steady Reynolds averaged Navior-Stokes equations are solved full turbulently to get the flow field of Trap wing model and DLR-F11 model with S-A turbulent model. It can be found from the numerical results that the consistency of numerical results between structured and unstructured grid is very good. The lift and drag coefficient from the numerical simulation in the linear region of the curve agree well with the experiment and some discrepancy exists in the non-linear region, which can be seen from the smaller lift coefficient and larger stall angle of the numerical results. The surface pressure coefficient along the span wise agree perfect with the experiment except the wing tip. The discrepancy is due to sensitivity of the flow field to the distribution of the grid near the wing tip, which can be learned from the conclusion of 1st AIAA High Lift Prediction Workshop. The rationality of the mesh generation and numerical method can be validated according to the simulating results of the two models and the needs for CFD simulation during aerodynamic design phases can be satisfied.

Reference

[1] Jeffrey P. Slotnick, Judith A. Hannon, “Overview of the First AIAA CFD High Lift Prediction Workshop,” AIAA Paper 2011-862.
[2] C. L. Rumsey, M. Long, R. A. Stuever and T. R. Wayman, “Summary of the First AIAA CFD High Lift Prediction Workshop,” AIAA Paper 2011-939.
[3] R. Rudnik and S. Melber-Wilkending, “DLR Contribution to the 2nd High Lift Prediction Workshop,” AIAA Paper 2014-0915.
[4] Thibaut Deloze and Eric Laurendeau, “NSMB contribution to the 2nd High Lift Prediction Workshop,” AIAA Paper 2014-0913.
[5] Yves Allaneau, Uri Goldberg, Sukumar Chakravarthy and Oshin Peroomian, “Contribution from Metacomp Technologies, Inc. to the Second High Lift Prediction Workshop,” AIAA Paper 2014-0912.